A Compact and High Throughput Reactor of Monolithic-Structured Catalyst Bed for Conversion of Syngas to Liquid Fuels

Wei Liu[1], Yong Wang, Wayne Wilcox, Shari Li, David King

Pacific Northwest National Lab (PNNL)

Abstract: Syngas conversion is needed for the production of liquid fuels and/or chemicals from renewable or remote feedstock at capacities much smaller than the conventional Fischer-Tropsch (F-T) plant. Here, we present a multiscale-engineered, modular-type design approach toward the development of a compact reactor unit to make syngas-to-liquids economically feasible at small scales. The fundamental design idea is tested by using a Re-Co/alumina catalyst coated on a monolith support of channel size about 0.9mm. 92~98% of one-pass CO conversion with <10 % of CH_4 selectivity is obtained with the structured bed under typical F-T reaction conditions. The gas superficial linear velocity was found as one critical parameter that may allow scale-up of the hydrodynamics from the small-scale laboratory tests directly to practical sizes of the reactor with the proposed design strategy. A pore wetness and surface perspiration model is proposed to explain the experimental data and rationalize the new design concepts.

Keywords: Fischer-Tropsch, multi-scale, gas to liquid, pore wetness, perspiration, catalyst design, reactor design, structure.

[1] Corresponding information: wei.liu@pnl.gov, 509-375-2524

Introduction

Syngas ($CO+ H_2$) is mostly produced from fossil fuels such as petroleum, coal, and natural gas in current industrial processes. It can also be derived from various renewable energy and/or hydrocarbon sources, such as biomass, industrial wastes, and municipal solid wastes. Catalytic conversion of syngas is one critical process technology for the production of liquid hydrocarbon fuels and/or chemicals from various carbon and hydrogen resources. Fischer-Tropsch (F-T) synthesis is a well-known industrial process for conversion of syngas to hydrocarbon liquid fuels. However, a conventional F-T plant is typically operated at high processing capacity[1-2] and integrated into a petrochemical and/or refinery complex to achieve scale economy. By contrast, most renewable energy and/or remote hydrocarbon resources are characteristic of small capacities and unstable supplies, and they are often distributed at various geographic locations. The conversion process becomes cost-prohibitive by using the conventional process technologies and plant designs at such a capacity scale that is orders of magnitude smaller than the typical petrochemical plant or oil refinery. In addition to the capacity-scale economy, operation flexibility such as quick unit turn-around from shutdown to start-up is necessary for distributed conversion units. Step-out catalytic processing technologies are needed for the world to obtain chemical feedstock and/or liquid fuels from diverse and renewable energy and/or hydrocarbon sources.

A great amount of research and development effort in the literature studies has been devoted to improvement of catalyst compositions and/ structures by utilizing new materials and state-of-the-art characterization tools. Examples in the catalyst design aspect include egg-shell catalyst beads for fixed beds[3], cobalt-based catalysts[4], iron-based catalyst[5], catalyst particles for slurry reactor[6], and new catalysts for product selectivity enhancement[7]. Fixed beds comprising

loading of catalyst beads into a reactor tube, fluidized beds, and slurry bubble columns are the commonly-employed reactor technologies[8-11]. Micro-channel reactor technologies have been proposed and explored to enhance heat and mass transfer by making characteristic transport dimensions substantially smaller than those in the conventional tubular reactor[12-14]. Overall, the literature reports on new reactor design ideas/principles have been scarce relatively to catalysis studies.

The F-T reactor itself represents only a small fraction of the capital cost in a conventional F-T plant design. As illustrated in Figure 1, the conventional F-T reactor typically produces a reaction mixture effluent containing a significant fraction of unconverted syngas and by products such as methane in addition to the desired liquid product. The unconverted syngas and methane have to be separated out of the product mixture and recycled back to the syngas generation process unit. The recycling system increases plant operation complexity, and incurs more energy consumption and capital cost. Since methane is a refractory compound for reforming reactions, the recycled gas significantly increases duty of the upstream process steps, reforming reaction, gas conditioning.

Present reactor and catalyst bed design concepts

The goal of our study is to develop a new reactor technology that enables essentially complete conversion of syngas in one pass without excessive production of methane and that leads to a compact reactor unit suitable for small-scale operation. The proposed process flow diagram is illustrated in Figure 2. The reactor is run under such conditions that >90% of syngas feed is converted. In this way, complicated and expensive recycling system is avoided. The reactor effluent is separated with relatively simple means into residual gas, liquid hydrocarbon fuels, and water. The residual gas containing H_2, CO, methane, and CO_2 can be combusted as a

fuel gas to provide energy to the unit operation, while the processing water can be re-used. The hydrocarbon mixture is lumped as a liquid-phase product outlet that can be transported to a centralized location, petrochemical plant or refinery for production of specific liquid fuels and/or chemical products.

Obviously, the reactor design is a critical challenge to realize the above process objectives. There must be good reasons why the current reactors are not run at complete one-pass conversion. To aid discussion of the proposed new reactor design concept, a simplified reaction network is given in Figure 3 to show characteristic of the syngas catalysis chemistry. The F-T synthesis is a surface catalyzed polymerization process that uses CH_x monomers, which are formed by hydrogenation of adsorbed CO molecules, to produce hydrocarbons with a broad range of chain length and functionality. In parallel to the desired polymerization reaction, methane can be produced by the methanation reaction, and water-gas-shift reaction may occur to produce CO_2. Coke can be produced from either CO decomposition or un-controlled polymerization reactions. Coking often causes catalyst deactivation[15-16]. The F-T reaction is highly exothermic and can easily run away if the temperature is not effectively controlled. The F-T reaction occurs under an environment of multiple physical phases and complex chemical compositions, which include liquid-phase hydrocarbons such as waxes, water, light hydrocarbons, inorganic gases (H_2, CO, CO_2), and solid catalysts. These are basic issues being considered for design and development of new reactor technologies.

In the authors' point of views, the limiting factors to run high one-pass conversion with conventional reactors could be (i) high CH_4 and CO_2 selectivity; (ii) balance between flow hydrodynamics and reaction kinetics, such as back mixing that makes high one-pass conversion

fundamentally impossible with a single-stage reactor; (iii) accelerated catalyst deactivation; (iv) lack of an effective catalyst; (v) effective temperature control of the catalyst bed.

Thus, a multi-scale design strategy is taken in this work to tackle these long-standing problems by decoupling convoluted factors [17,18]. The proposed reactor design principles are illustrated in Figure 4. A monolithic-structured catalyst bed is employed in planar heat exchanger-type configuration. Each layer of the reaction zone is arranged adjacent to two heat exchanging zones. The layers can be repeated to the desired height. Different from the micro-channel approaches, the spacing of a reaction zone in the proposed design may be range from 5 to 30cm, i.e., at macro-scales. Thus, the existing material processing technologies can be utilized to fabricate such kind of reactor modules. The structured catalyst bed is the core of the reactor design. The structured bed comprises an array of parallel catalytic reaction channels of channel size at 0.3 to 3.0mm levels. The mini-structured bed can be made by conventional, low-cost material processing methods, such as ceramic monoliths made by extrusion. A syngas feed stream is introduced from the top slit of the reaction zone and distributed uniformly over the structured bed. A porous membrane sheet may be placed on the top of the structured bed to serve as a gas distributor. The gas stream flows downwards through individual catalytic reaction channels. The reacted product is collected at the bottom slit of the reaction zone and the resulting product stream is discharged out of the reactor. The reaction heat generated from the catalyst bed is transported to the cooling/reaction interface through convective flows in the feed and product slits.

This reactor design approach allows decoupling of design parameters at different scales. The reactor-scale design can focus on aspects of flow distribution, cooling flow arrangement, heat exchange efficiency between the reaction and cooling layer, mechanical integrity of the

reactor vessel, and mitigation of thermal and pressure stresses. In a single reaction zone, the mini-structured bed serves both as a catalyst support and as a three-dimensional thermal conduction matrix. The reaction heat generated at a reaction channel can be spread by thermal conduction through the support. Compared to point-to-point contacts in a conventional bead-packed catalyst bed, the continuous solid support structure should provide good thermal conduction. Thus, the bed-scale design can address issues of thermal conductivity, open-frontal area fraction, and channel size and geometry.

The catalyst structure and mass transfer between the catalytic sites and the bulk flow can be handled by the channel-scale design. Figure 5a shows one representative reaction channel. The catalyst is coated on the channel wall, syngas flows into the channel, and the produced liquid drips off the channel wall and comes out of the channel along with the gas flow. The flow patterns for the bead-packed fixed bed and a bubble slurry reactor are drawn in respective Figures 5b and-c for comparison.

As outlined in Figure 6, a series of elemental mass transfer steps are involved in an actual catalytic conversion process. The reactants (CO and H_2) need to transport from the bulk flow to the catalytic sites, while the reaction products (Oil, H_2O, CH_4) need to be transported from the catalytic sites back into the bulk flow. In the catalytic reaction channel, the pore diffusion and catalyst loading can be managed by controlling thickness and pore structures of the catalyst coating layer, while the external mass transfer can be controlled by flow conditions (Ug, U_l) and channel geometry. A salient feature of the structured reaction channel[19] is the possibility to achieve uniform gas/liquid/catalyst contacting, plug flow, and high external mass transfer rates, as compared to the bead-packed bed and slurry bubble column. In the bead-packed bed, segregation of the gas and catalyst at the particle scale is inevitable due to random stacking of

particles and trap of the liquid product among inter-particle voids. In the bubble slurry column, the catalyst particles may be uniformly dispersed in the liquid-phase product, but there would be significant back-mixing of the product and syngas bypass.

Design parameters at the reactor and reaction-zone scales should be well simulated by computer modelling based on the design and material structures studied in the related fields, such as heat exchangers and diesel particulate filters. The catalytic channel reaction performance, which is the fundamental of the proposed reactor design, is experimentally tested.

Experimental testing of fundamental design ideas

Catalyst preparation. Catalytic materials and compositions used in this work were demonstrated for the F-T reaction in our previous work[13,20]. The commercial cordierite monolith substrate was used to construct the structured catalyst bed. Three major steps involved in preparation of a monolithic catalyst were alumina slurry batching, alumina coating, and catalyst impregnation. The alumina coating slurry was prepared in the following procedure. 100 mesh acidic Al_2O_3 powder (Engelhard) was mixed with de-ionized water. Polyacrylic acid (PAA) with molecular weight of 2000 g/mol (Sigma–Aldrich) was added as an electrostatic dispersant. pH of the slurry was adjusted within the range of 3-4 by adding HNO_3 solution. Then, polyvinyl alcohol (PVA) (Aldrich) and Lgepol C0-720 (Sigma–Aldrich) were added as a binder and surfactant, respectively. Furthermore, poly ethylene glycol (PEG) (Sigma–Aldrich) with molecular weight of 2000 g/mol was added as a plasticizer. The resulting slurry batch had typical compositions of about 30 wt.% alumina, 0.2 wt.% PAA, 1.0 wt.% PVA, 1.0 wt.% PEG, and 0.1 wt.% Lgepol. The whole mixture was ball milled for 16-48 hrs to obtain homogenous slurry.

The slurry was coated on the monolith support of 1cm diameter x 7.5cm long by a dip coating technique, i.e., quick contacting of the monolith with the coating slurry. The coating was

repeated three times with inter-stage drying at 100^{o}C. Finally, the coated monolith was calcined at 550^{o}C for 4 h at 5^{o}C/min ramp rate for removal of all the organics and adhesion of the alumina coating layer onto the support. On average, the alumina coating loading was 16.0 wt%.

The active catalyst phase was dispersed on the alumina coating with impregnation technique. The impregnation solution was prepared by dissolving cobalt nitrate hexahydrate (98% purity, Aldrich), perrhenic acid (Engelhard), and lanthanum nitrate hydrate into de-ionized water. The monolith was wetted o incipient wetness by the solution. The wetted monolith was dried in air at 90^{o}C overnight and followed by calcinations at 350^{o}C for 3 h. The impregnation was repeated to obtain targeted catalyst loadings. The resulting Co, Re, and La loading on the alumina coating was 17.8 wt. %, 3.3 wt. %, and 3.0 wt. %, respectively. The total catalyst metal loading on the alumina basis was 24.1 wt. %, while the catalyst loading (metal +alumina) in the whole monolith piece was 19.2 wt%.

For comparative testing, alumina-supported F-T catalyst particles were prepared by using the same raw materials, procedures, and conditions as described above.

Catalytic reaction tests. Schematic of the reactor system used in this work was shown in Figure 7. The monolith catalyst module was inserted into a ½" OD reactor tube of suitable ID so that the gap between the tube wall and the monolith was comparable or less than the channel size. This way of packing was necessary to minimize bypass of the flow along the channel wall. The monolith catalyst was positioned in the middle of the reactor tube by two thermocouples at the top and bottom. Thus, no other material was loaded into the reactor during testing of monolith catalysts. The reactor tube was wrapped by an oil jacket to control the reaction temperature, and the temperatures were measured at the bottom and top of the catalyst bed.

For testing of catalyst particles, the catalyst particle was packed in the middle of a reactor tube by using SiC particles. Similar to the reactor configuration for the monolith catalyst bed, the thermocouple wells were placed at the top and bottom of the catalyst bed, respectively; and the reactor tube was sheathed in an oil jacket for temperature control.

All the catalysts were activated by reduction in hydrogen prior to introduction of the syngas. After the catalyst was reduced at about 400^{o}C for 12 hours at 0.1MPa of H_2, the reactor temperature was cooled down under flowing hydrogen. Then, the reactor was pressurized to 25 bars with 5% H_2 in helium. A syngas feed with H_2/CO ratio of 2, unless specifically noted, was introduced. 3 to 4 vol. % of Ar was spiked into the feed both as an internal standard and for purge purpose. The reactor temperature was raised to the target value at 1^{o}C/min. Hydrocarbon and water in the reactor effluent were condensed in a chilled vessel under pressure. Non-condensed gases were analyzed using an on-line gas chromatograph (Agilent QUADH G2981A with Molsieve 5A, PoraPlol Q) to determine CO conversion and light product selectivity. The condensed liquid products were analyzed in a HP 6890 connected with a DB-5 column. The olefinic compounds were identified by GC-MS (HP 5973C), then quantified by a GC (HP 6890). Conversion and selectivity are calculated based on the product gas analysis for CO, CO_2, CH_4, C_2H_4, C_2H_6, C_3H_6, C_3H_8, and C_4.

CO conversion is calculated by the following equation:

$$X_{CO} = \frac{F_{in,0} \cdot x_{CO,in} - F_{ex,0} \cdot x_{CO,,ex}}{F_{in,0} \cdot x_{CO,in}} \qquad (1)$$

Selectivity toward to molecule i on carbon number basis is calculated as follows:

$$S_i = \frac{F_{ex,0} \cdot x_{i,ex} \cdot n_i}{X_{CO} \cdot F_{in,0} \cdot x_{CO,in}} \qquad (2)$$

Weight-hourly space velocity is calculated based on CO mass feed rate for characterize the catalyst activity:

$$WHSV = \frac{m_{CO}}{W_{Cat}} \quad (3)$$

Superficial gas linear velocity based on the reactor entrance condition is used to characterize the channel flow conditions:

$$U_g = \frac{F_{in,0} \cdot T_{top}}{T_0 \cdot P \cdot A_R \cdot 60} \quad (4)$$

Experimental results and discussion

Catalyst coating. Uniformity of the catalyst coating on the monolith support was examined by Scanning Electron Microscopy (SEM) and Energy-dispersive X-ray spectroscopy (EDS) analysis. The coating surface texture and cross-section are shown in Figure 8. The channel surface is fully covered by the catalyst, even though there are mud cracks on the coating. Presence of a catalyst coating layer is evident in the cross-sectional view. The channel opening is about 0.9mm, while the catalyst coating thickness is about 30 to 70μm. The EDS analysis shows presence of Al, Si, Co, Re, and La elements. The Al and Si are attributed to the support, while Co, Re, and La are impregnated catalyst metals. Presence of the catalyst metals on the channel wall surface and at the middle point of the coating layer is confirmed. The SEM/EDS analyses provide compositions at the localized spots. For a given global composition, variation of the compositions among different spots is possible.

Reaction uniformity among monolith channels. For structured beds, uniform flow distribution and reaction in all catalyst channels is a critical factor for effective catalyst utilization and for minimization of side reactions. To check this, the reactor was quenched after the reaction testing by stopping the feed gas flow and circulating cold silicone oil. The

morphology of two spent monolith pieces unloaded from the reactor is shown in Figure 9. All the channels facing the feed syngas in the upper piece of the monolith catalyst are fully open. The monolith piece looks uniform, indicative to uniformity of the catalyst deposition and reaction. The un-coated support would look grey, and the white wax would be trapped if there was stagnant or dead space. All the channels in the lower piece of the monolith are filled with white wax on the bottom, which indicate that the reaction (formation of wax) occurred among all the channels. These observations suggest that the feed gas was distributed evenly among the catalyst channels by simple stacking of two pieces of the monolith catalysts.

Exceptional performances of the monolithic-structured catalyst bed. Steady-state reaction performances of the structured bed are shown by plots in Figure 10. First of all, the temperature control was excellent. Given about 150mm of the bed height, the top and bottom temperatures of the catalyst bed are consistent, and their differences are typically less than 2^{o}C at high CO conversion levels. Superficially, the bottom bed temperature could be much higher than the top bed due to exothermic reactions in the confined catalyst channels. The small temperature difference observed from the experiments can be explained by the thermal conduction through the monolith support matrix and rapid heat transfer between the silicone oil and reactor tube. The gap between the reactor tube wall and monolith body apparently did not impose limitation to the radial heat transfer. This result confirms the possibility of the temperature control at a larger spacing of the reaction zone in the proposed reactor design (Figure 4) than the diameter of conventional tubular reactors, certainly orders of magnitude larger than the micro-channel reactor spacing.

The structured bed had a quick response to changes of the reaction conditions, and showed fairly good stability. The steady-state reaction could be reached within a few hours.

Possibility to reach high CO conversion levels without excessive production of CH_4 and CO_2 is clearly shown. The reactor was started with a syngas feed of H_2/CO =1.6 containing 3.9 vol. % Ar as an internal standard. Figure 10 shows about 79% CO conversion, which corresponds to nearly complete H_2 conversion. The higher CO conversion during the transient period was due to the inventory hydrogen in the reactor system prior to the syngas introduction, since the catalyst was pre-reduced in H_2 gas. After the feed H_2/CO ratio was adjusted to stoichiometric ratio of 2.0, about 95-98% of CO conversion occurred under the same temperature, pressure, and space velocity. Since the CO conversion was so high, nearly all the feed H_2 and CO gas was consumed and we had difficulty to maintain the reactor pressure with a very small flow of remaining Argon gas. It should be noted that the methane and CO_2 selectivity were only about 8 % and 2 %, respectively. After the space velocity was doubled, under the same temperature and pressure, the CO conversion was dropped to about 68%, the CH_4 selectivity increased to about 9.5 %, while the CO_2 selectivity decreased to less than 0.5 %. Decline of the CO % conversion with increasing space velocity can be explained by reduced residence time. However, variations of the CH_4 and CO_2 selectivity with the space velocity could not be explained based on residence time.

To elucidate reaction behaviour of the structured bed, the reactor was loaded with other two monolith catalyst pieces and tested under various reaction conditions after the steady-state line-up. Excellent temperature control and >95% one-pass CO conversion at (CH_4 +CO_2) selectivity less than 10 % were reproduced. Variations of CO conversion, CH_4 selectivity, and CO_2 selectivity with reaction temperature under constant reactor pressure are plotted in Figure 11. The temperature is an average of the top and bottom bed readings. Several data points were collected in a steady-state operation under each set of conditions, and the average values are plotted. The closed symbols in Figure 11 are for WHSV of 2.0 1/h, while the open ones

correspond to WHSV of 4.1 1/h. For a given WHSV, the CO conversion, CH_4 selectivity, and CO_2 selectivity all increase with temperature. This is expected from the reaction kinetics. However, comparison at different WHSVs tells a different story. At the same temperature, the CO conversion and CO_2 selectivity at the higher WHSV are lower than those values at the lower WHSV, which is in line with reaction kinetics. The CH_4 selectivity shows a very different behaviour. At the same or similar temperature, the CH_4 selectivity at the higher WHSV is the same or higher than values at the lower WHSV. Obviously, such a variation cannot be explained based on correlation of conversion with residence time.

The un-usual selectivity behaviour is explained by channel flow hydrodynamics under different reaction conditions. The flow conditions inside the channel are characterized by the gas superficial linear velocity under the reactor entrance conditions. It is recognized that the gas flow inside the channel would diminish while the liquid flow gradually increases along the channel depth. Variations of CO conversion, CH_4 selectivity, and CO_2 selectivity with the superficial gas velocity are shown in Figure 12, where the closed symbols and open symbols are for 225^{o}C and 210^{o}C reaction temperature, respectively. For a given temperature, the CO conversion decreases with increasing the gas velocity. This is explained by reduced residence time, since the catalyst bed height was fixed. The CO_2 selectivity decreases with increase of the gas linear velocity. However, the CH_4 selectivity tends to increase with the gas linear velocity. The high CO conversion and low CH_4 selectivity are achieved at the low gas linear velocity. The gas linear velocity becomes one critical design parameter for the proposed reactor concept. Thus, the plate-like catalyst bed configuration is presented in Figure 4. Such a bed would allow low gas linear velocities at high gas feed flow rates. The hydrodynamic pattern inside the catalyst channel could be very complex, due to presence of multiple phases. The proposed design allows scaling

of the channel flow hydrodynamics from the small-scale laboratory reactor to any size of the reactor.

Performances of catalyst particle beds. For comparison purposes, the line-out behaviour of particle-loaded catalyst beds is shown in Figure 13. The same monolith catalyst as used above was crushed and sieved into 60-200 mesh (~170um). The crushed particle was loaded into a reactor tube and sandwiched by a layer of SiC particles on the top and bottom. The crushed particle bed was started in the same procedure as used for the structured bed. Figure 13a shows variations of CO conversion, CH_4 selectivity, and CO_2 selectivity with time on stream. The top and bottom bed temperatures were maintained constantly at 210^{o}C. However, it took a much longer time to reach the conversion plateau than the structured bed. The CO conversion declined with time, while the CH_4 selectivity increased with time. These trends suggest that formation of CH_4 is favoured on the deactivated catalyst. The CO_2 selectivity was very low. The crushed monolith catalyst particle represents an egg-shell catalyst structure, i.e., an active catalyst layer coated on an inert support. Comparative testing results of fully-catalyzed catalyst particles are shown in Figure 13b to further show performance characteristic of the particle-loaded catalyst bed. This catalyst particle of + 200 mesh size (~45μm) was prepared with the same materials and same procedures as used for the preparation of the catalyst coatings on the monolith. The catalyst particle was loaded into a reactor tube with the SiC particle diluent at volume ratio of 1:1. It was experienced that the catalyst bed temperatures varied erratically at the beginning of testing and made it difficult to control the bed temperature. The initial data points show nearly 90% CO conversion and about 5 % CH_4 selectivity. However, as the bed temperatures got stabilized at 210^{o}C, the CO conversion declined and the CH_4 selectivity increased with time. These trends point out the same conclusion as conjectured with the crushed

monolith particle bed that the deactivated catalyst causes lower CO conversion and higher CH_4 selectivity.

Comparison of the structured bed to the particle bed. To avoid complication of the catalyst preparation, the same monolith catalyst in the structured bed is compared to the crushed particle bed in Figures 14a and –b. At the same reaction temperature, Figure 14a shows that the structured bed gives much higher steady-state CO conversion than the crushed particle bed. The CO conversion activity of the structured bed is about four times that of the crushed particle bed. The CH_4 selectivity for the crushed particle bed decreased with increasing space velocity. The increase of the CH_4 selectivity with space velocity for the structured bed was explained above attributed to the increased gas superficial linear velocity. The structured bed also showed a higher CO conversion activity than the crushed particle bed at a higher temperature. Figure 14b shows that under constant space velocity, the CO conversion and CH_4 selectivity increase with temperature for both beds. Even though the space velocity for the structured bed is about two times of the crushed particle bed, the CO conversion with the structured bed is significantly higher than the crushed particle bed.

A plot of CH_4 selectivity versus CO conversion is used to compare the CH_4 selectivity of different catalyst beds. By excluding transient data points, data points at different aging times and different space velocities at temperature about 210^oC are plotted in Figure 15. I can be seen that the CH_4 selectivity increases proportionally with the CO conversion for both the crushed particle and catalyst particle bed. The CH_4 selectivity would become too high to be practical if that trend is extrapolated to high CO conversion levels, such as >90%. This selectivity versus conversion paradox is breached by using the structured bed. Figure 15 shows that the CH_4

selectivity can be controlled below 10% at about >95% of CO conversion. Clearly, the un-usual behaviour of the structured bed calls for a new reaction engineering model.

Pore wetness and surface perspiration model for F-T reaction. This work reveals dramatic impacts of the catalyst bed design and operation on F-T reaction performances for a given catalyst material. Clearly, the F-T reaction activity, selectivity, and stability are not merely a catalysis problem, i.e., tailoring of catalyst pore structures, compositions and active sites. The ways how a catalyst is loaded into a reactor vessel and tested play a significant role in the resulting reaction performances. Based on our research results and literature analysis, we propose a new model to guide the F-T reactor designs and operation, as depicted in Figure 5a. Characteristic of the proposed model and preferred catalyst bed designs is discussed in the following three aspects.

(i) **Structured mini-channel flow to have a plug flow pattern and avoid any dead/stagnant space in the bed.** The plug flow is necessary to eliminate any back-mixing and achieve high one-pass conversion. Minimization of the dead space would be helpful to prevent the catalyst deactivation from excessive reactions -coking.

(ii) **Fully-wetted catalyst pores to prevent the catalyst surface from formation of dry or hot spots.** Methane formation on a dry catalyst can be very fast, due to fast gas diffusion and rapid heating up of the local spots. The reaction can easily run away on a dry catalyst. When the catalyst pore is wetted by a liquid fluid, diffusion rates of H_2 and CO reactants are slowed down and thermal conductivity of the catalyst is significantly enhanced. F-T reaction kinetics is slower than methanation. Thus, the pore wetness would quench the methanation reaction without significant reduction of the F-T reaction rate. During a dynamic reaction process, the pore wetness is determined by the formation rate of the liquid product and drying (or liquid

evaporation) rate. For a given temperature and pressure, the drying rate will be affected by the gas flow rate inside the channel. Thus, the gas linear velocity inside the channel should be controlled below a certain level in order to keep the catalyst surface stay wet. This mechanism explains the decreased methane selectivity with decreasing gas linear velocity, which is observed in this work.

(iii) **Discharge of the liquid product from the catalyst pore through perspiration to avoid coverage of the catalyst surface by a thick liquid layer**. If the liquid product needs to be washed away from the catalyst surface, a thick liquid layer could be formed that may drastically reduce diffusion rate of H_2 and CO gas from the channel flow into the catalyst pore. In a perspiration process, the catalyst surface can stay wet without a thick liquid layer on majority of the surface. The product liquid perspired from the catalyst pore gradually accumulates on the catalyst surface and coalesces into a droplet. The droplet is dislodged from the catalyst surface by gravity and/or by gas dragging when it grows to a certain size. This mechanism explains four times of the higher CO conversion activity obtained with the structured bed than with the crushed particle bed. Since the same catalyst material was used, the enhanced activity must result from enhanced external mass transfer of H_2 and CO, i.e., mass transfer from the bulk flow onto the catalyst external surface. The pore diffusion length in the structured bed should be the same as in the crushed particle, because the catalyst coating was fixed. Even though the crushed particle provides a much higher geometric surface area for external mass transfer than the channel surface in the structured form, there could be a smaller effective gas/liquid mass transfer area and/or thicker liquid film in the packed bed of the crushed particle than in the structured channel. This is explained with the illustration in Figure 5b. The liquid trapped in the inter-particle voids may become stagnant so that there is no ideal

gas/liquid/particle contact on individual particle basis. In a random-packed particle bed, the catalyst particles behave as an aggregate, cluster or a group. The equivalent size of such an aggregate would depend on the bed packing and reaction conditions, and could be orders of magnitude larger than the individual particle size.

The physical model presented here can be further elaborated with mathematical equations in the future work. This reaction engineering model and the structured bed design would be applied to syngas-to-liquid conversion processes other than the F-T reaction. Effective temperature control, high CO conversion activity, and low CH_4 selectivity are common performance characteristic for a gas-to-liquid conversion process. In this work, we use one catalyst material and monolithic support to elucidate the structured bed design ideas. The materials and structures of both catalyst and support can certainly be optimized to enhance the reaction performance of the structured bed. For example, a monolithic support of the higher geometric surface area and more catalyst loading can be used to increase the reactor throughput. The monolithic support can be made of metallic or ceramic materials.

5. Conclusion

Structured catalyst bed & reactor design concepts are presented in this work to address long-term dilemma for the gas-to-liquid catalytic reaction process, better temperature control, better catalyst activity and stability, lower CH_4 selectivity, ease for scale-up. For the given catalyst material and catalysis chemistry, all these problems are fundamentally related to mass and heat transfer at different scales. The proposed approach provides a way for decoupling of convoluted design parameters so that different aspects of the reactor design and operation problems can be tackled through designs at the reactor-scale, catalyst bed-scale, and individual channel-scale, respectively.

The fundamental idea of the proposed reactor design is demonstrated for the F-T catalytic reaction by using known catalyst and support materials, a Re-Co/alumina catalyst coated on a cordierite monolith support. At a H_2/CO feed ratio of 2, ~95% CO conversion and <10% CH_4 selectivity was obtained with the monolithic-structured bed. The structured bed shows about four times of higher CO conversion activity than the crushed particle bed of the same catalyst. These levels of high CO conversion and low CH_4 selectivity were not obtainable by using the conventional particle bed. The gas superficial linear velocity was found as one critical design and operation parameter for the structured bed. This funding makes it possible to scale up hydrodynamics directly from small laboratory-bench testing units to practically any sizes with the proposed reactor design configuration.

The pore wetness and surface perspiration model is proposed to explain the present experimental results and observations, and to rationalize new reactor designs for gas-to-liquid reaction processes.

Acknowledgment

This work was supported under laboratory-directed research and development (LDRD) program of PNNL by Energy Conversion Initiative and Energy & Environmental Directorate.

Pacific Northwest National Laboratory (PNNL) is operated by Battelle for the Department of Energy. This work was partially supported by PNNL Energy Conversion Initiative.

Nomenclature

A_R = cross-sectional area of reactor tube, cm^2

$F_{in,0}$ = Feed gas flow rate under standard gas conditions, sccm

$F_{ex,0}$ = Residual gas flow of reactor effluent after the liquid condenser, sccm

m_{CO} = mass flow rate of CO fed into the reactor, g/h

n_i = number of carbon atoms in molecule specie i, i=1 for CO_2 and CH_4.

P = reactor pressure, bar

S_i = Selectivity toward gas specie i, i = CH_4, CO_2, C_2H_4, C_2H_6, C_3H_6, or C_3H_8

T_{top} = Reactor top bed temperature, K

T_0 = temperature under standard gas conditions, 293K

U_g = superficial gas linear velocity under reactor entrance conditions, cm/s

W_{cat} = Net catalyst weight (alumina + metals), g

$x_{CO,ex}$ = Molar fraction of CO in residual gas

$x_{CO,in}$ = Molar fraction of CO in feed gas

$x_{CO,in}$ = Molar fraction of CO in feed gas

$x_{CO,ex}$ = Molar fraction of CO in residual gas

$x_{i,ex}$ = Molar fraction of molecule i in residual gas

X_{CO} = conversion of CO

Literature cited

1. Hoek A. 2003. The Shell middle distillate synthesis process Facts, Technology and Perspective. Presentation at CatCon2003, Houston, May 5-6th.
2. Sehabiague L, Lemoine R, Behkish A, Heintz YJ, Sanoja M, Oukaci R, Morsi BI. Modeling and optimization of a large-scale slurry bubble column reactor for producing 10000 bb/day of Fischer-Tropsch liquid hydrocarbons. J. of the Chinese Institute of Chemical Engineers. 2008; 39:169-179.
3. Iglesia E, Soled SL,Baumgartner JE, Reyes SC. Synthesis and catalytic properties of eggshell cobalt catalysts for the Fischer-Tropsch synthesis. J. of Catal. 1995; 153:108-122.
4. Iglesia E. Design, synthesis, and use of cobalt-based Fischer-Tropsch synthesis catalysts. Appl. Catal. A: General. 1997; 161: 59-78.
5. Dasgupta, D, Wiltowski T. Enhancing gas phase Fischer-Tropsch synthesis catalyst design. FUEL. 2011; 90 (1): 174-181.
6. Bukur DB, Carreto-Vazquez VH, Victor H, Ma WP. Catalytic performance and attrition strength of spray-dried iron catalysts for slurry phase Fischer-Tropsch synthesis. Applied Catalysis A-General. 2010; 388 (1-2):240-247.
7. Zhang QH, Kang JC, Wang Y. Development of Novel Catalysts for Fischer-Tropsch Synthesis: Tuning the Product Selectivity. CHEMCATCHEM. 2010; 2 (9): 1030-1058.
8. Sie ST, Krisha R. Fundamentals and selection of advanced Fischer-Tropsch reactors. Appl. Catal. A. 1999; 186:55-70.
9. Hulet C, Clement P, Tochon P, Schweich D, Dromard N, Anfray J. Literature Review on Heat Transfer in Two- and Three-Phase Bubble Columns. International Journal Of Chemical Reactor Engineering. 2009; 7: Art. No. R1.
10. Lu XJ, Hildebrandt D, Liu XY, Glasser D. Making Sense of the Fischer-Tropsch Synthesis Reaction: Start-Up. Industrial & Engineering Chemistry Research. 2010; 49 (20): 9753-9758.
11. Zhu XW, Lu XJ, Liu XY, Hildebrandt D, Glasser D. Study of Radial Heat Transfer in a Tubular Fischer-Tropsch Synthesis Reactor. Industrial & Engineering Chemistry Research. 2010; 49 (21): 10682-10688.
12. Lee M, Rumbold SO. Industrial microchannel devices –where are we today? First International Conference on Microchannels and Minichannels, ICMM2003-1101, Rochester, New York, USA, April 24-25, 2003.
13. Cao C, Hu J, Li S, Wilcox W, Wang Y. Intensified Fischer-Tropsch Synthesis Process with Microchannel Catalytic Reactors. Catal. Today. Catalysis Today. 2009; 140:149–156.
14. Knochen J, Guttel R, Knobloch C, Turek T. Fischer-Tropsch synthesis in milli-structured fixed-bed reactors: Experimental study and scale-up considerations. Chemical Engineering and Processing. 2010; 49 (9): 958-964.

15. Tsakoumis NE, Ronning M, Borg O, Rytter E, Holmen A. Deactivation of cobalt based Fischer-Tropsch catalysts: A review. Catalysis Today. 2010; 154 (3-4): 162-182.

16. Nam I, Seo JG, Hwang S, Song IK. Deactivation behaviors of hybrid Fischer-Tropsch catalysts in the production of middle distillate from synthesis gas in a dual-bed reactor. Research on Chemical Intermediates. 2010; 36 (6-7): 685-692.

17. Li J, Kwauk M. Exploring complex systems in chemical engineering – the multi-scale methodology. Chem. Eng. Sci. 2003; 58:521-535.

18. Liu W. Multi-scale Catalyst Design. *Chem. Eng. Sci*. 2007; 62: 3502-3512.

19. Liu W. Mini-Structured Catalyst Bed for Gas-Liquid-Solid Multiphase Catalytic Reaction. *AIChE J. 2002;*48(7): 1519-32.

20. Liu W, Hu J, Wang Y. Fischer-Tropsch Synthesis on Ceramic Monolith-structured Catalysts. Catal. Today. 2009 ; 140: 142–148

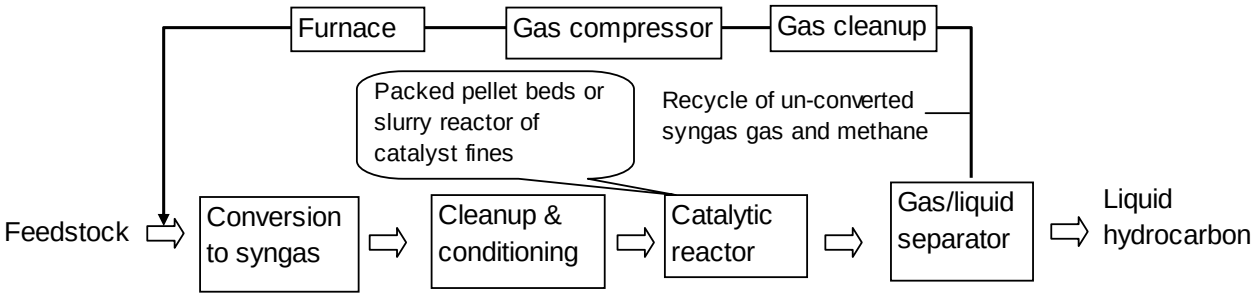

Figure 1. Process flow diagram with conventional F-T reactors

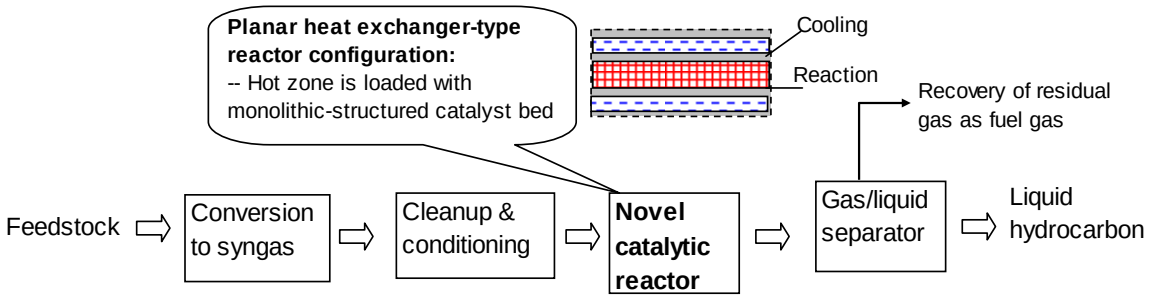

Figure 2. Simplified process flow diagram with proposed reactor technology

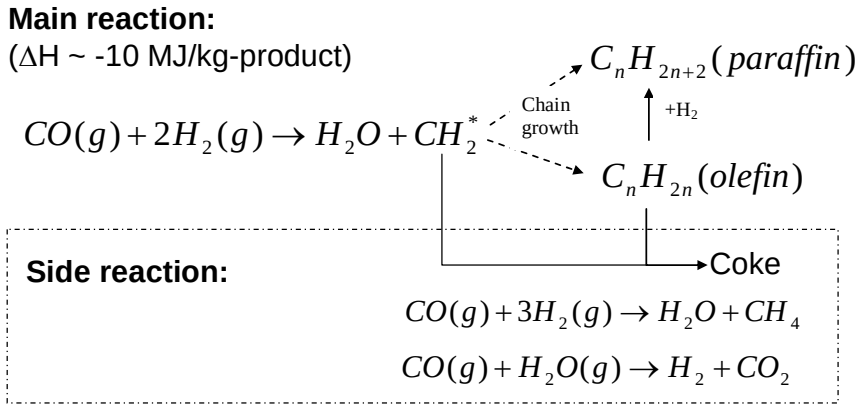

Figure 3. Major reaction paths under F-T reaction conditions

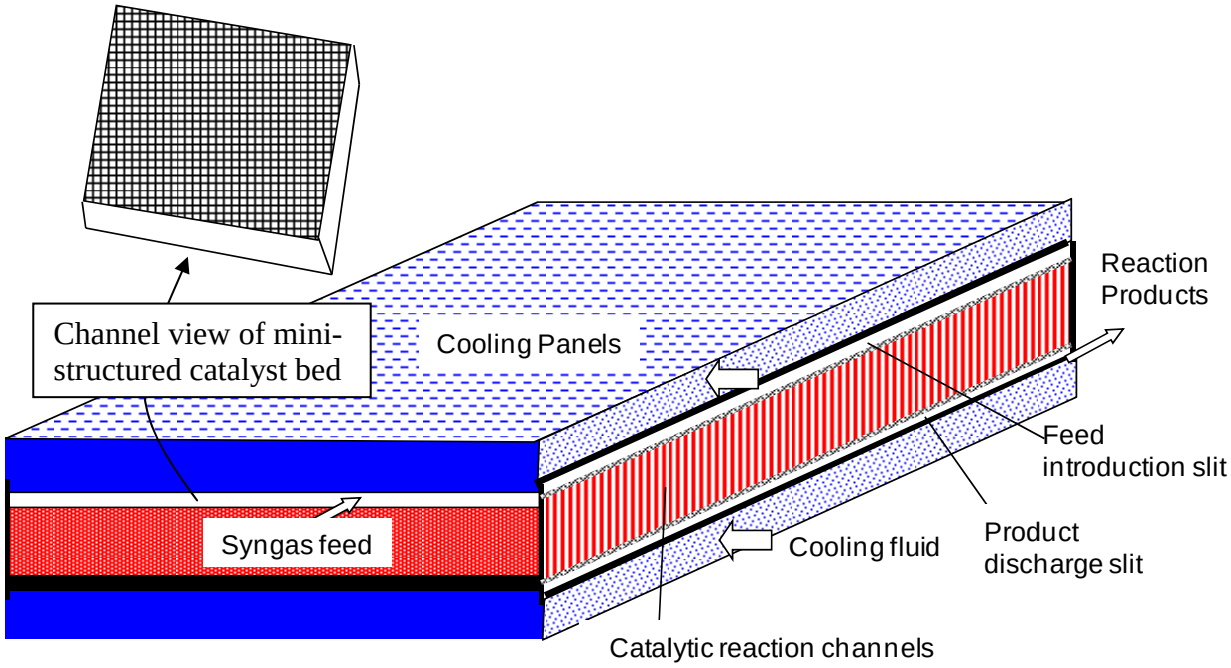

Figure 4 Schematic of multi-scale engineered reactor module proposed in this work

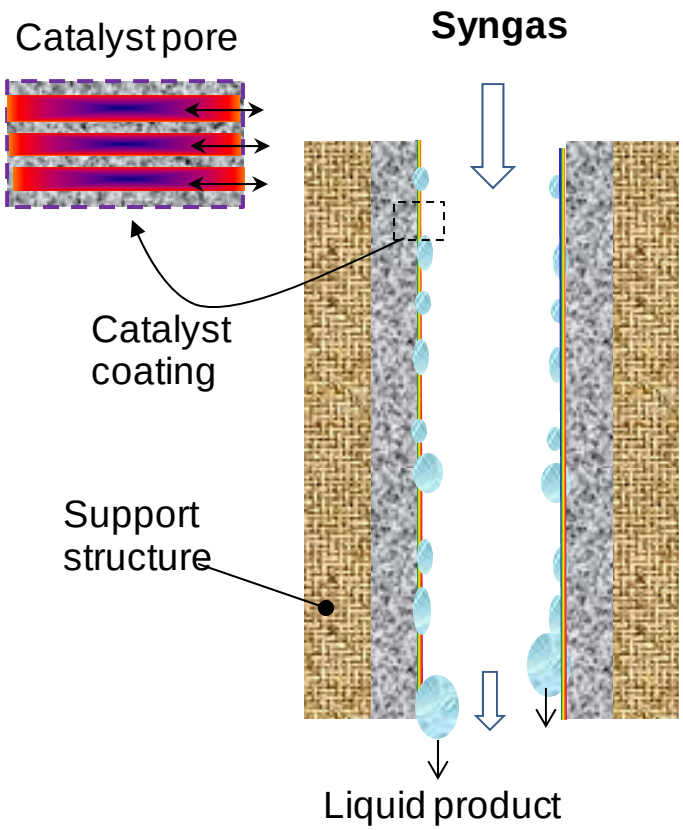

(a). Proposed channel flow reaction model

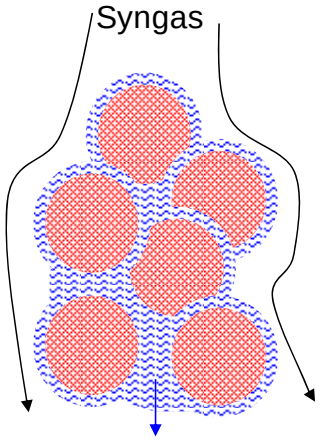

(b) Packed catalyst beads (or particles)

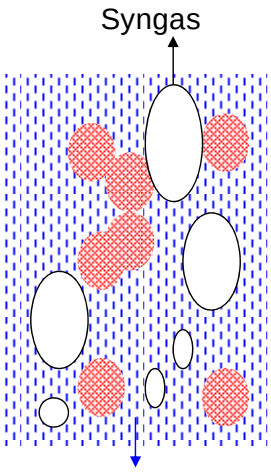

(c) Slurry bubble column

Figure 5. New reaction engineering model in comparison to other catalyst beds

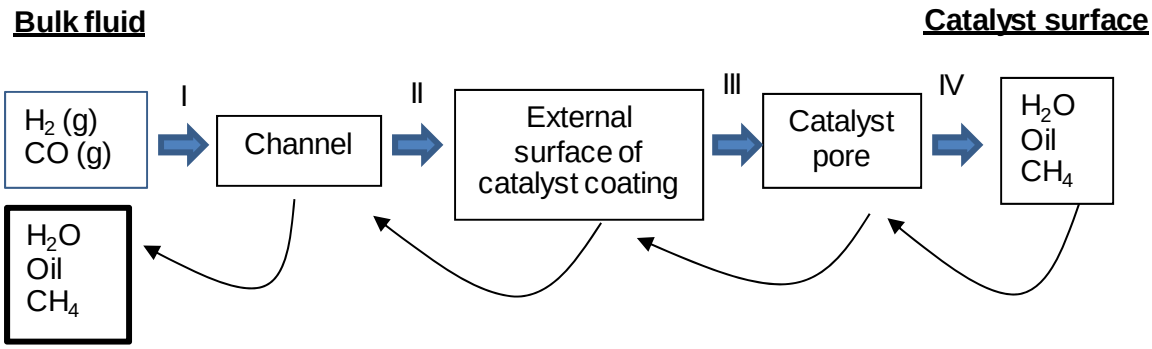

Figure 6. Elemental steps involved in a catalytic syngas conversion process

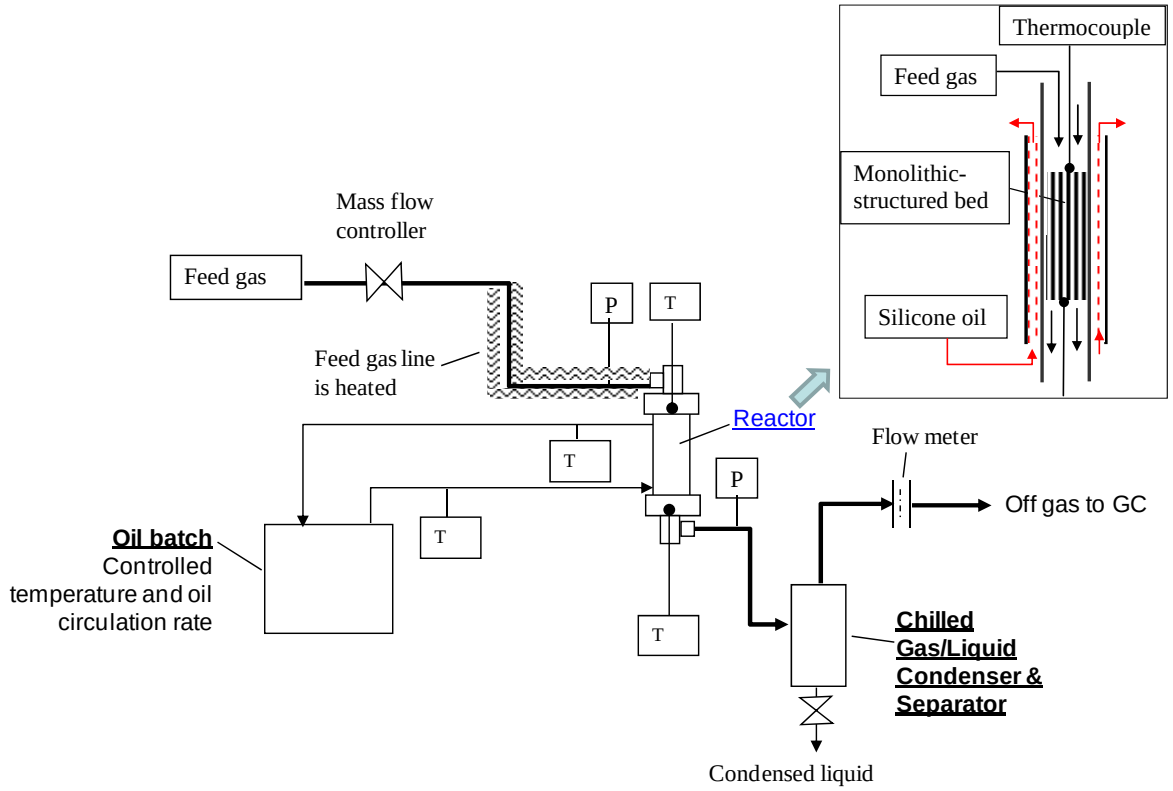

Figure 7. Schematic of reactor testing apparatus used in this work

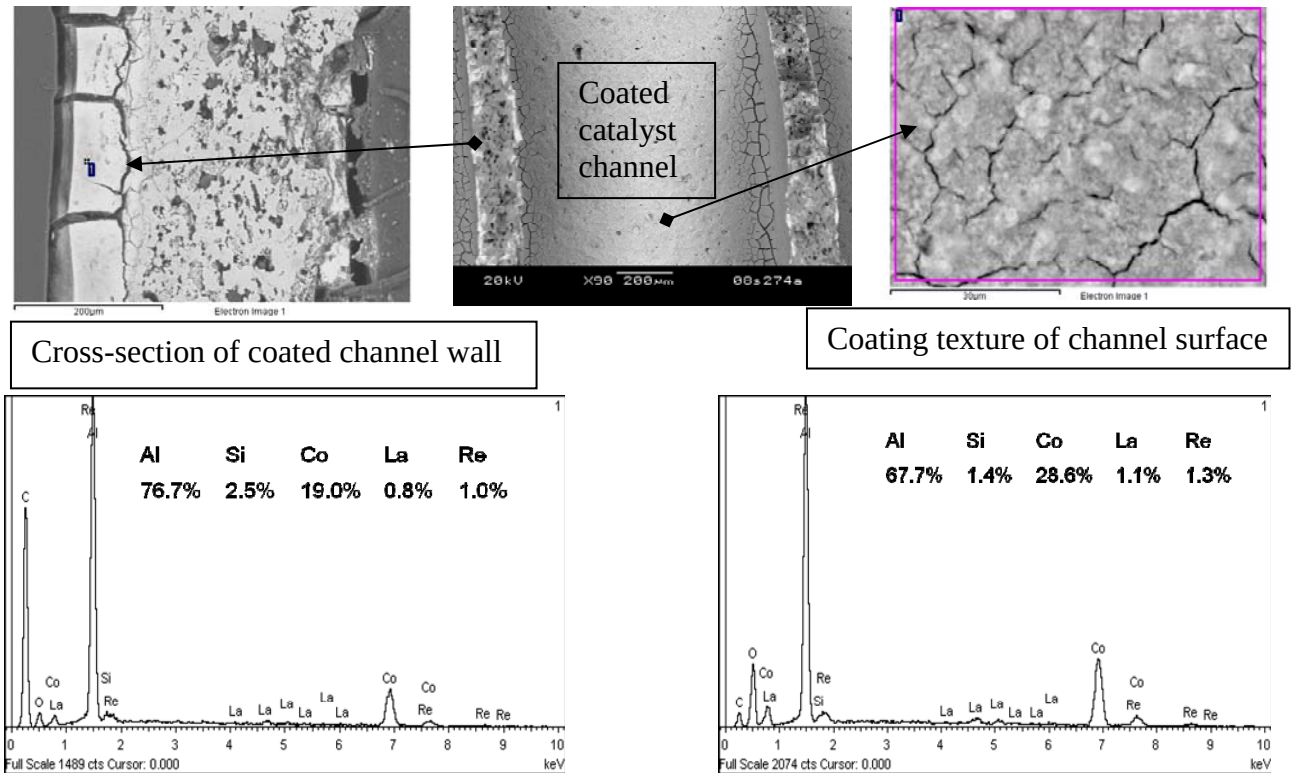

Figure 8. Structure and composition of F-T catalyst coating on Cordierite monolith channel

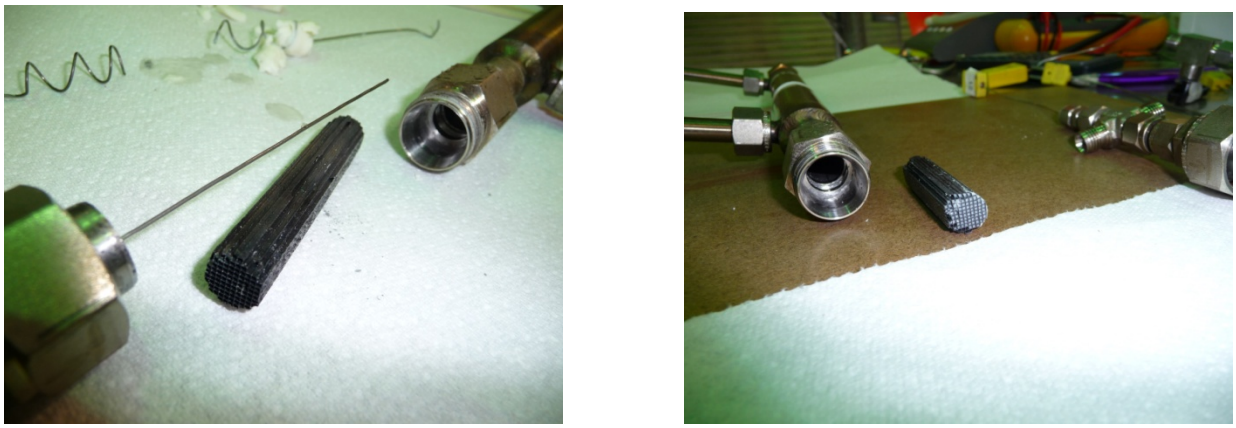

(a). Upper piece (b) Lower piece

Figure 9. Morphologies of monolith catalyst pieces after 45-day testing

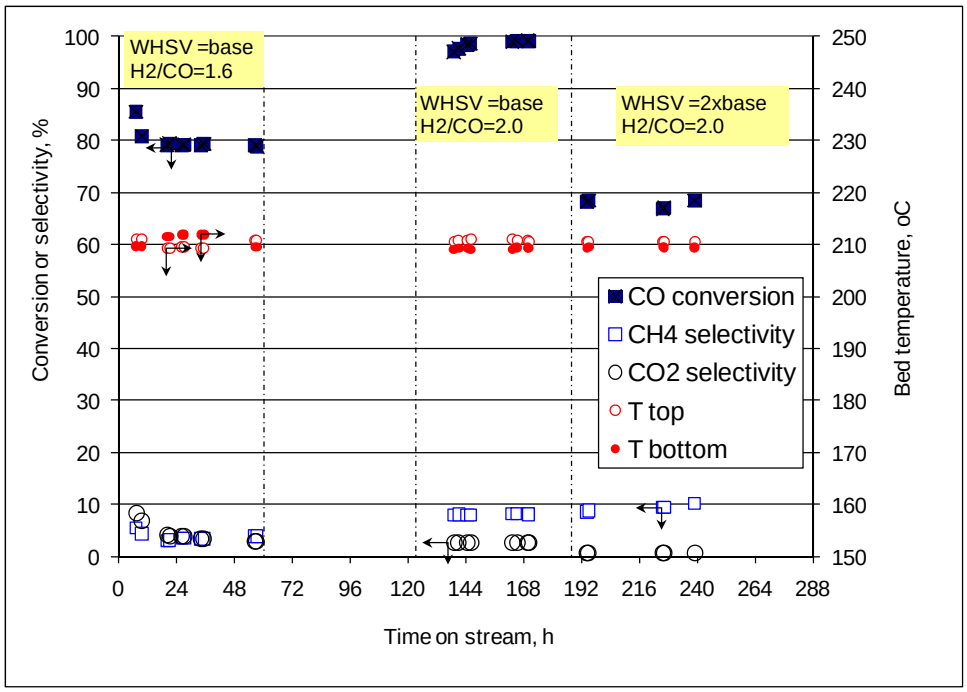

Figure 10. Steady-state performance of structured catalyst bed (25 bar)

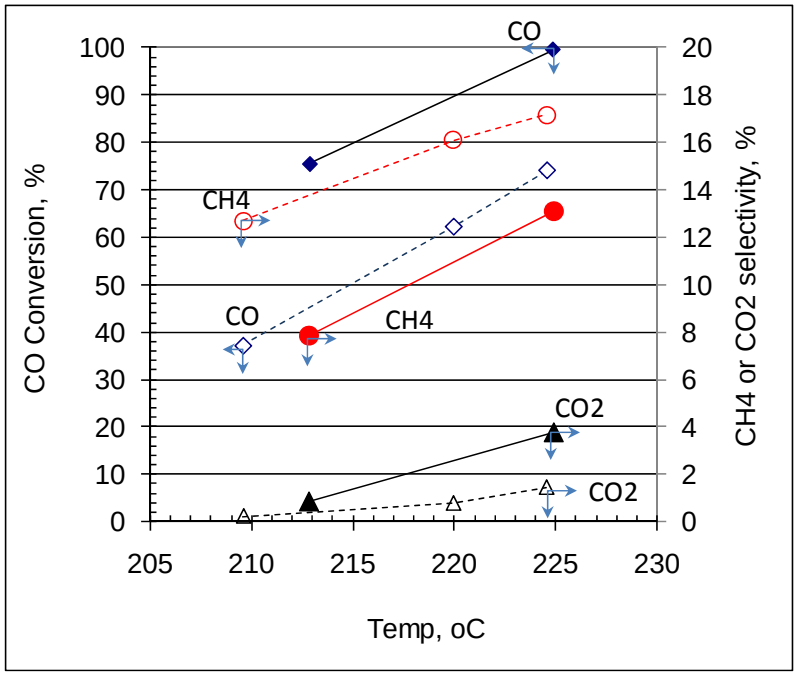

Figure 11 Impact of reaction temperature on performance of structured catalyst bed (feed H_2/CO ratio of 2:1, reactor pressure of 25 bar). Closed symbols for WHSV=2.0 1/h. Open symbols for WHSV=4.1 1/h

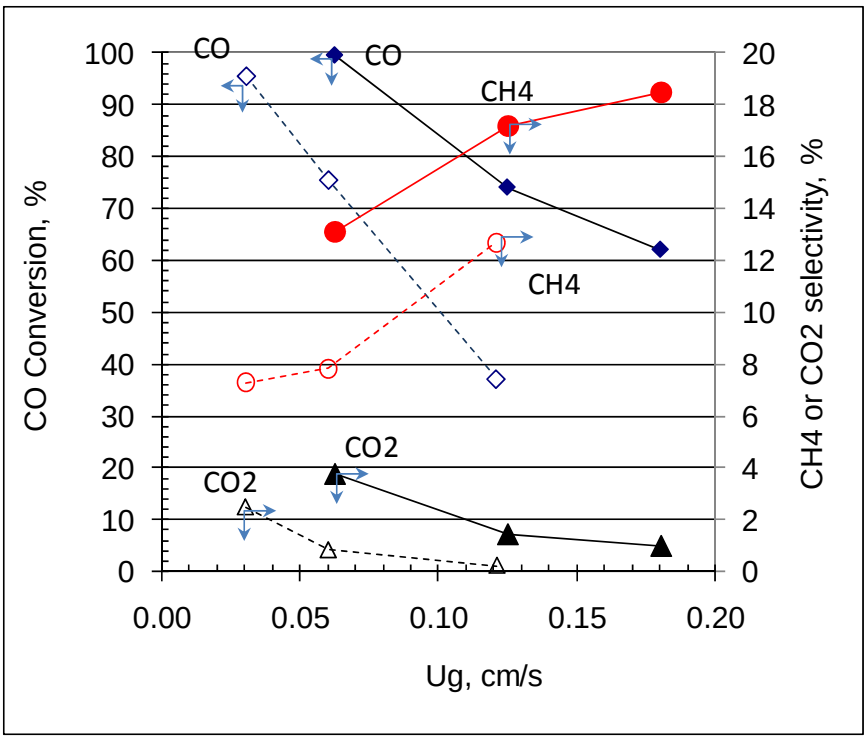

Figure 12. Impact of feed gas superficial linear velocity on performance of structured catalyst bed (feed H_2/CO ratio of 2:1, reactor pressure of 25 bar). Closed symbols for reaction temperature of 225^{o}C. Open symbols for 210^{o}C.

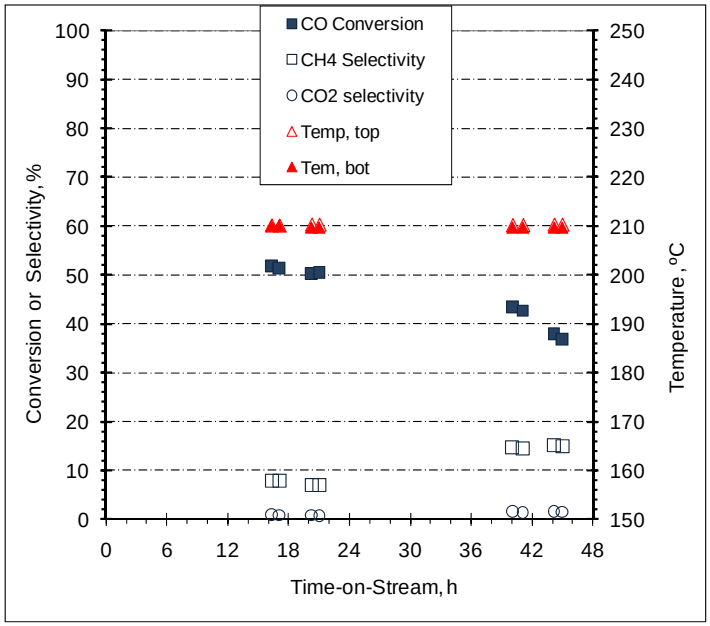

(a) Crushed monolith particle (WHSV=1.0)

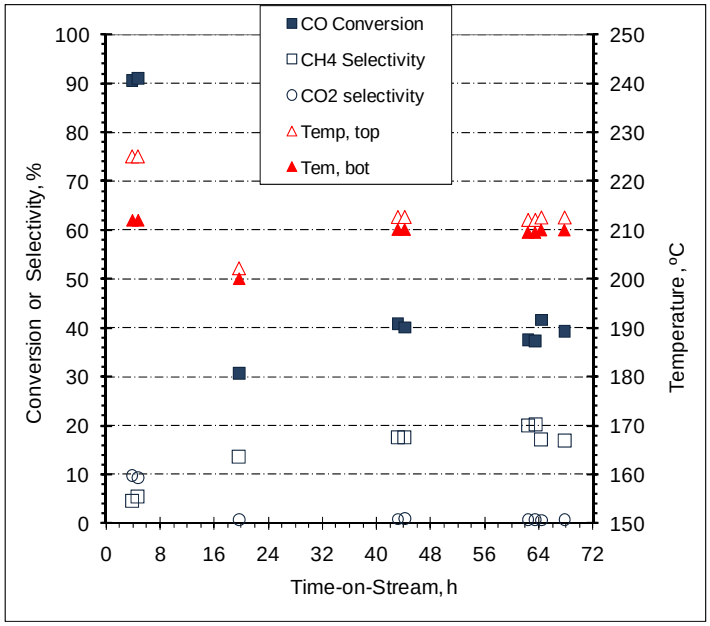

(b) Full-catalyzed catalyst particles (WHSV=0.9)

Figure 13. Performances of particle-loaded bed under steady-state reaction conditions (feed H_2/CO ratio of 2:1, reactor pressure of 25 bar).

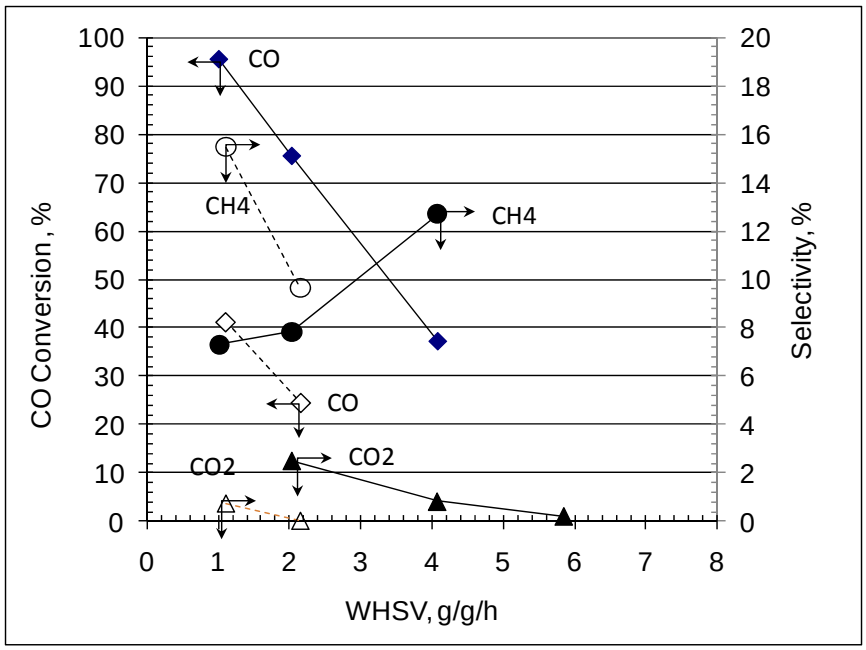

(a) 210°C

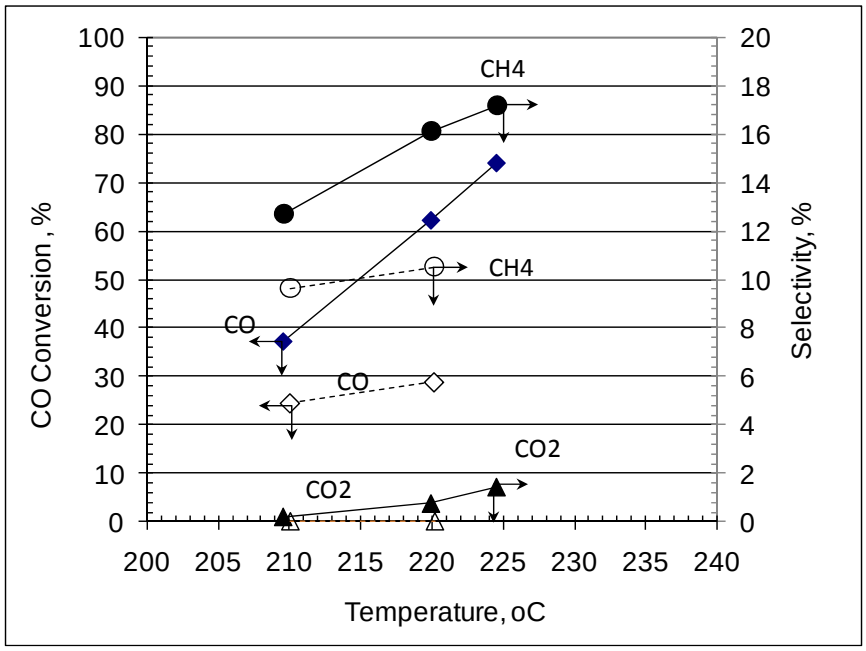

(b) WHSV=4.1 1/h for structured bed and WHSV=2.1 1/h for crushed particle

Figure 14. Comparison of monolith catalyst in structured bed to particle-loaded bed of its crushed particle (feed H_2/CO ratio of 2:1, reactor pressure of 25 bar). Closed symbols for the structured bed. Open symbols for the particle bed.

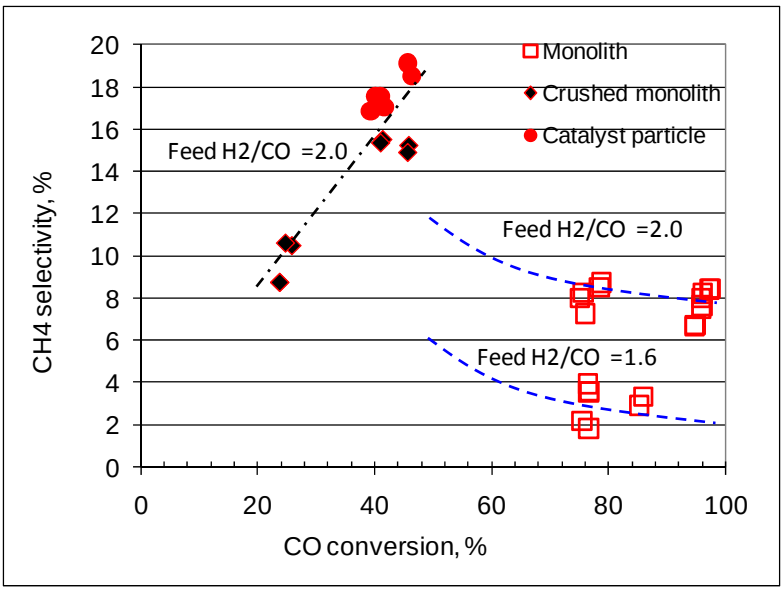

Figure 15. Variation of CH_4 selectivity with CO conversion (feed H_2/CO ratio of 2:1, 210^oC, reactor pressure of 25 bar).